Prediction of adsorption equilibria of water-methanol mixtures in zeolite NaA by molecular simulation

Tamás Kristóf

Molecular Simulation
Journal of
Experimental Nanoscience

Taylor & Francis
Taylor & Francis Group

Prediction of adsorption equilibria of water-methanol mixtures in zeolite NaA by molecular simulation

Journal:	*Molecular Simulation/Journal of Experimental Nanoscience*
Manuscript ID:	GMOS-2006-0106.R1
Journal:	Molecular Simulation
Date Submitted by the Author:	24-Jul-2006
Complete List of Authors:	Kristóf, Tamás; Pannon University, Dept. Phys. Chem.
Keywords:	mixture adsorption, molecular simulation, selectivity

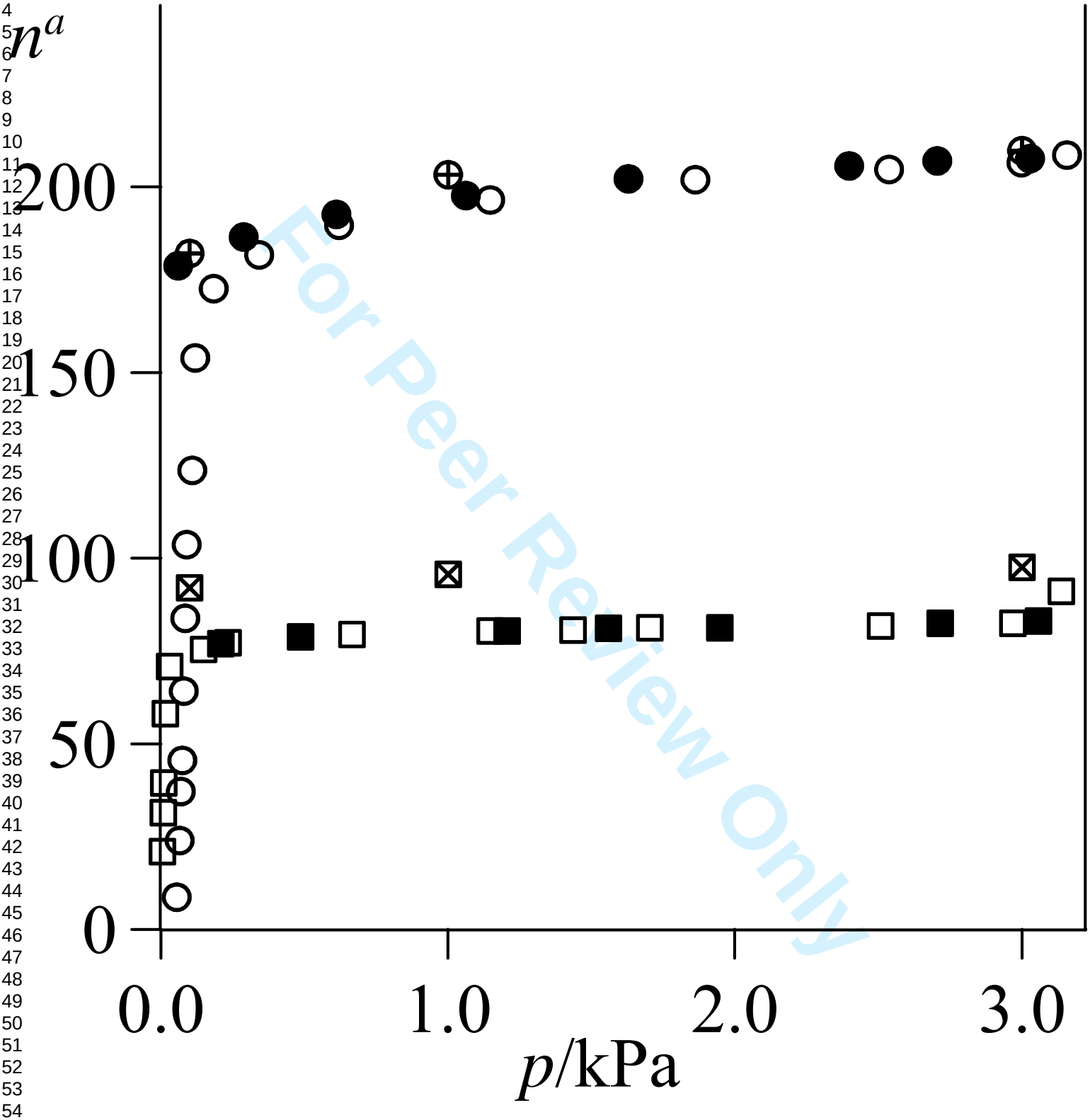

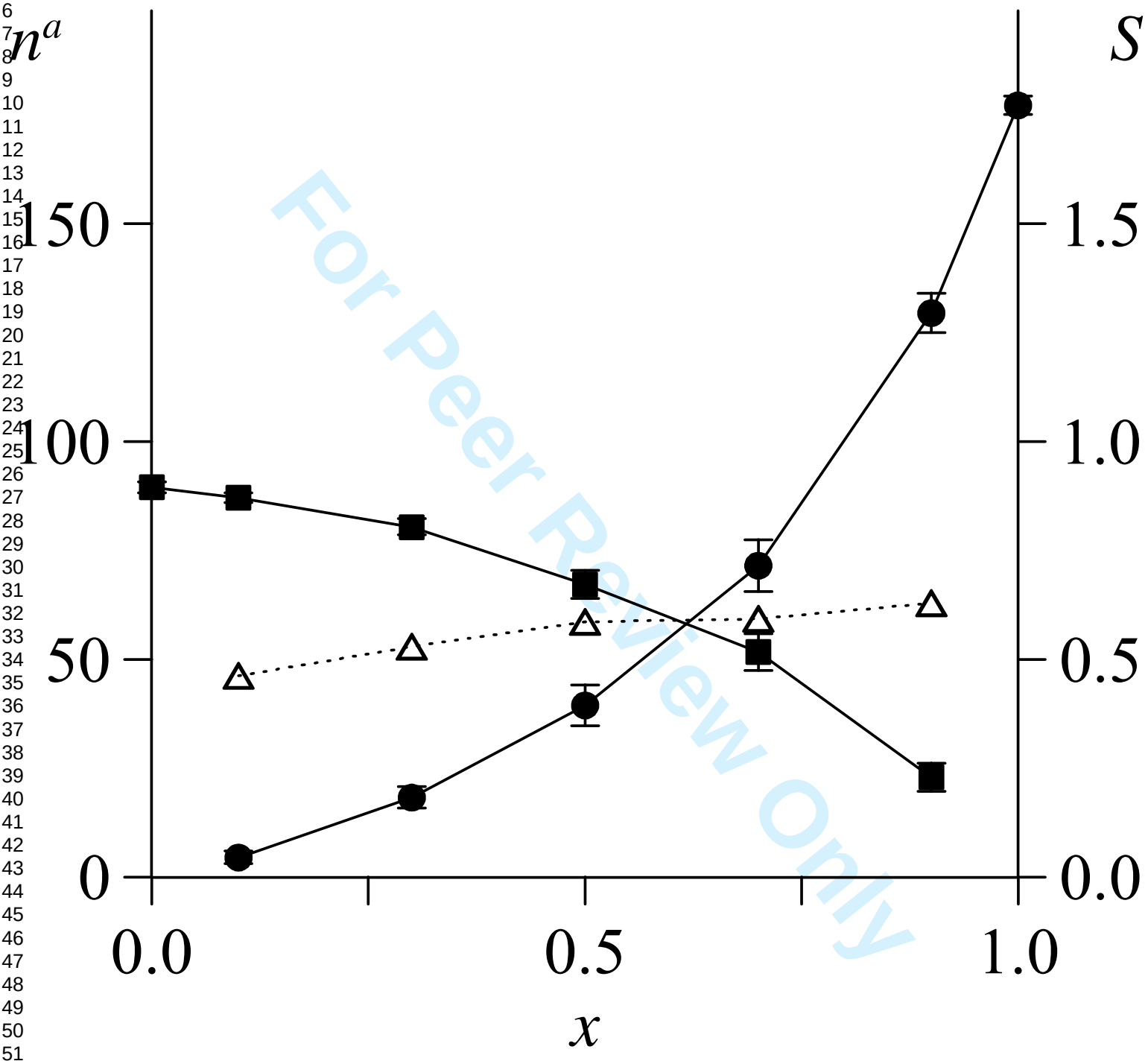

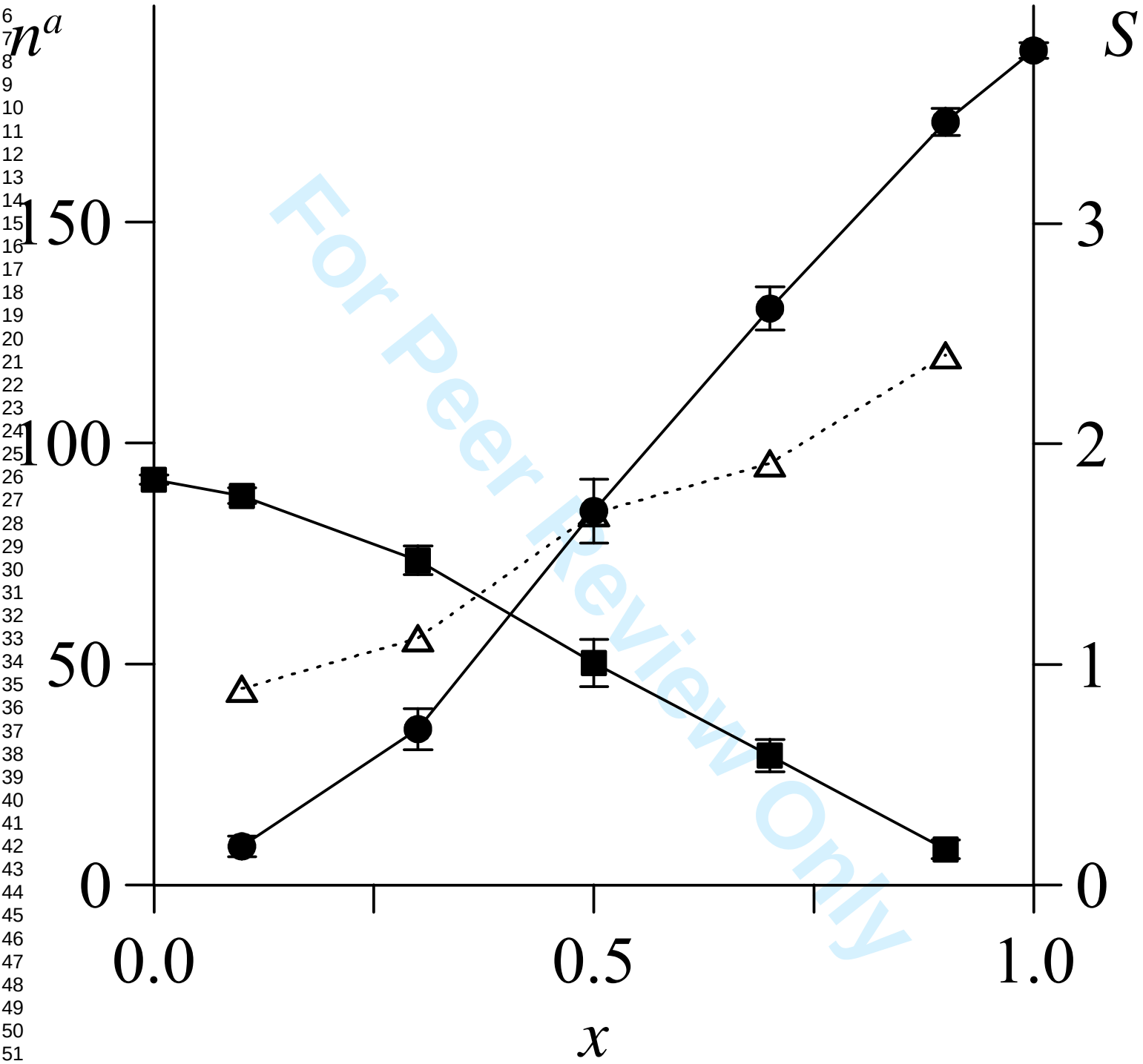

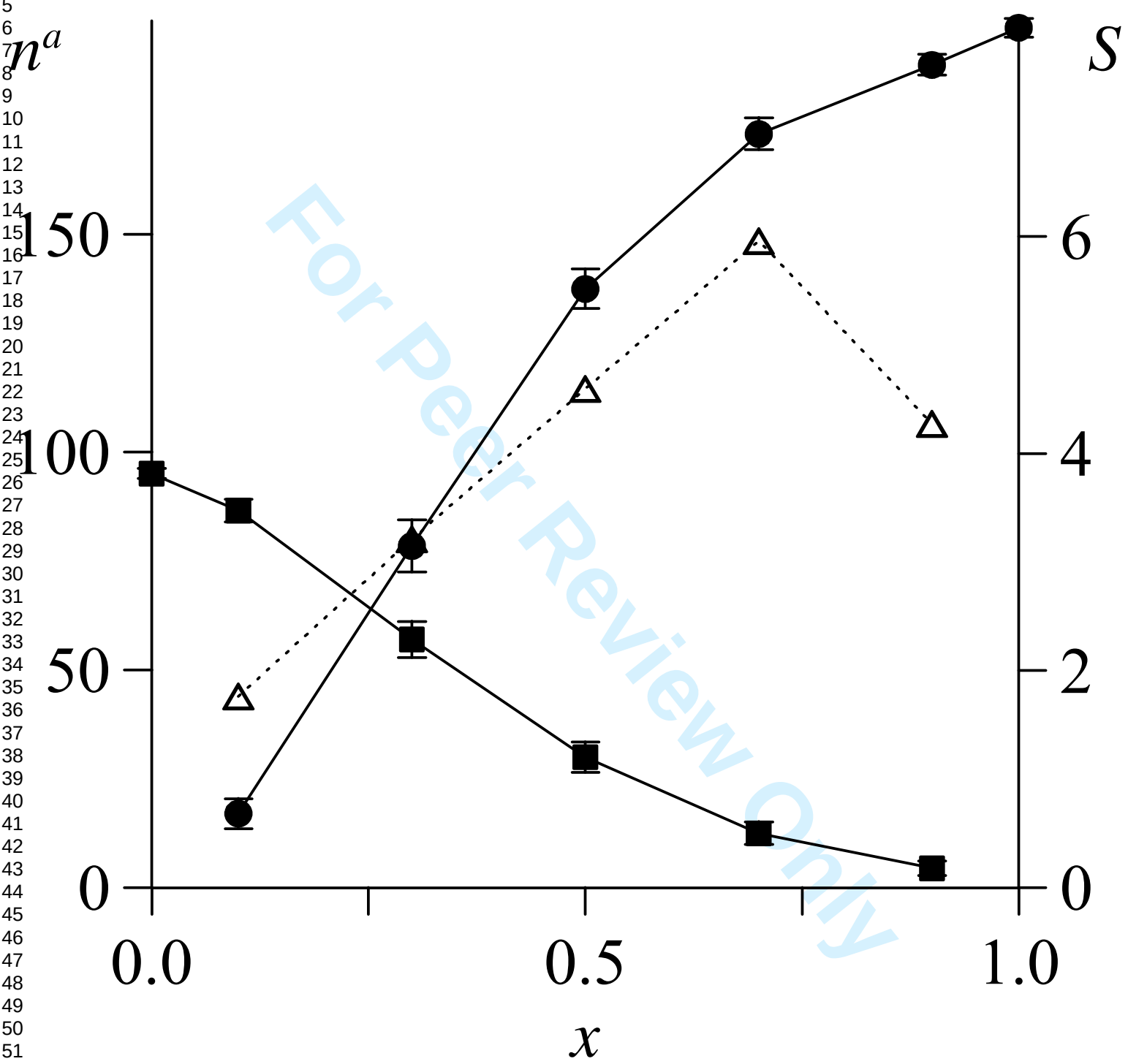

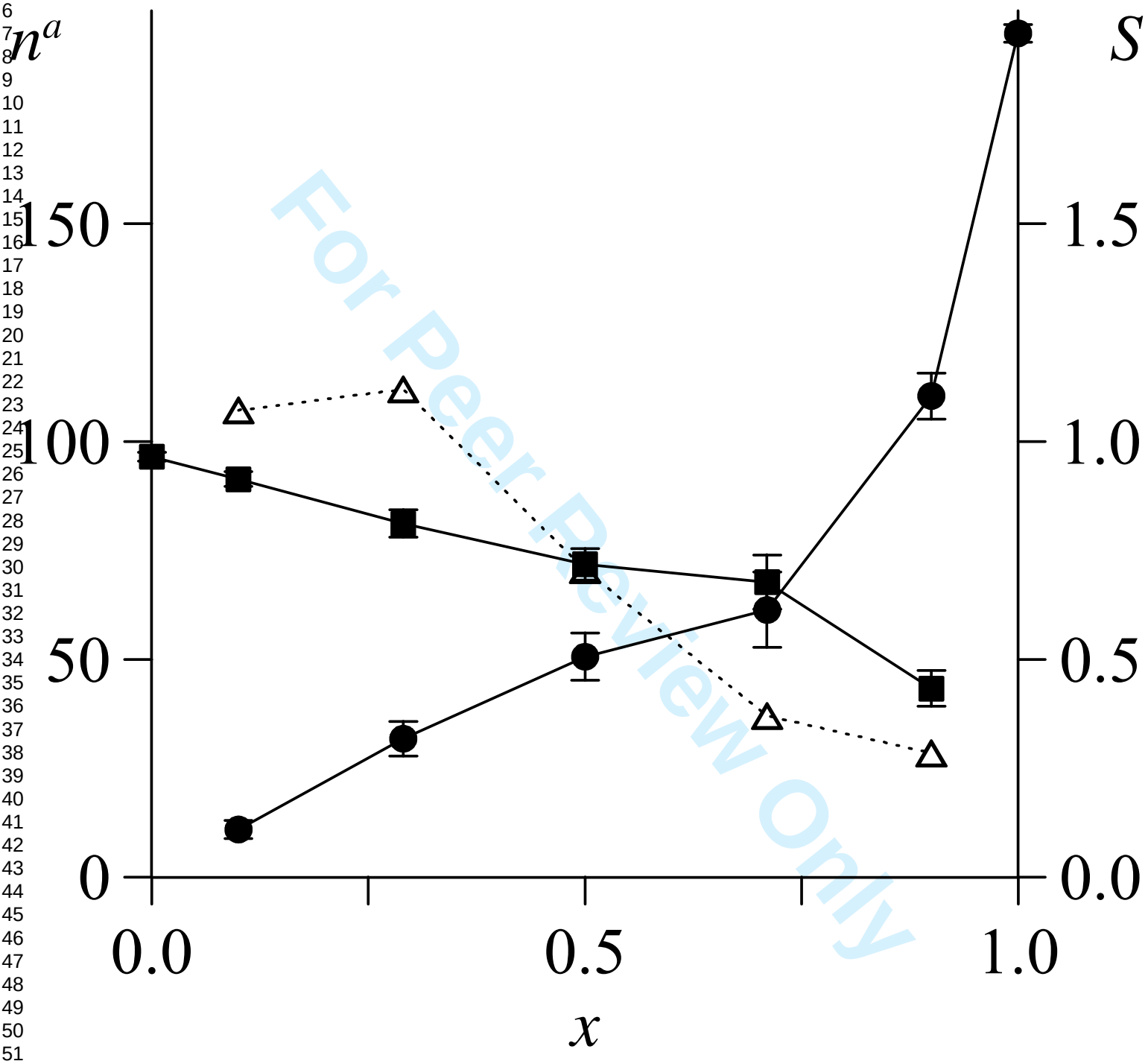

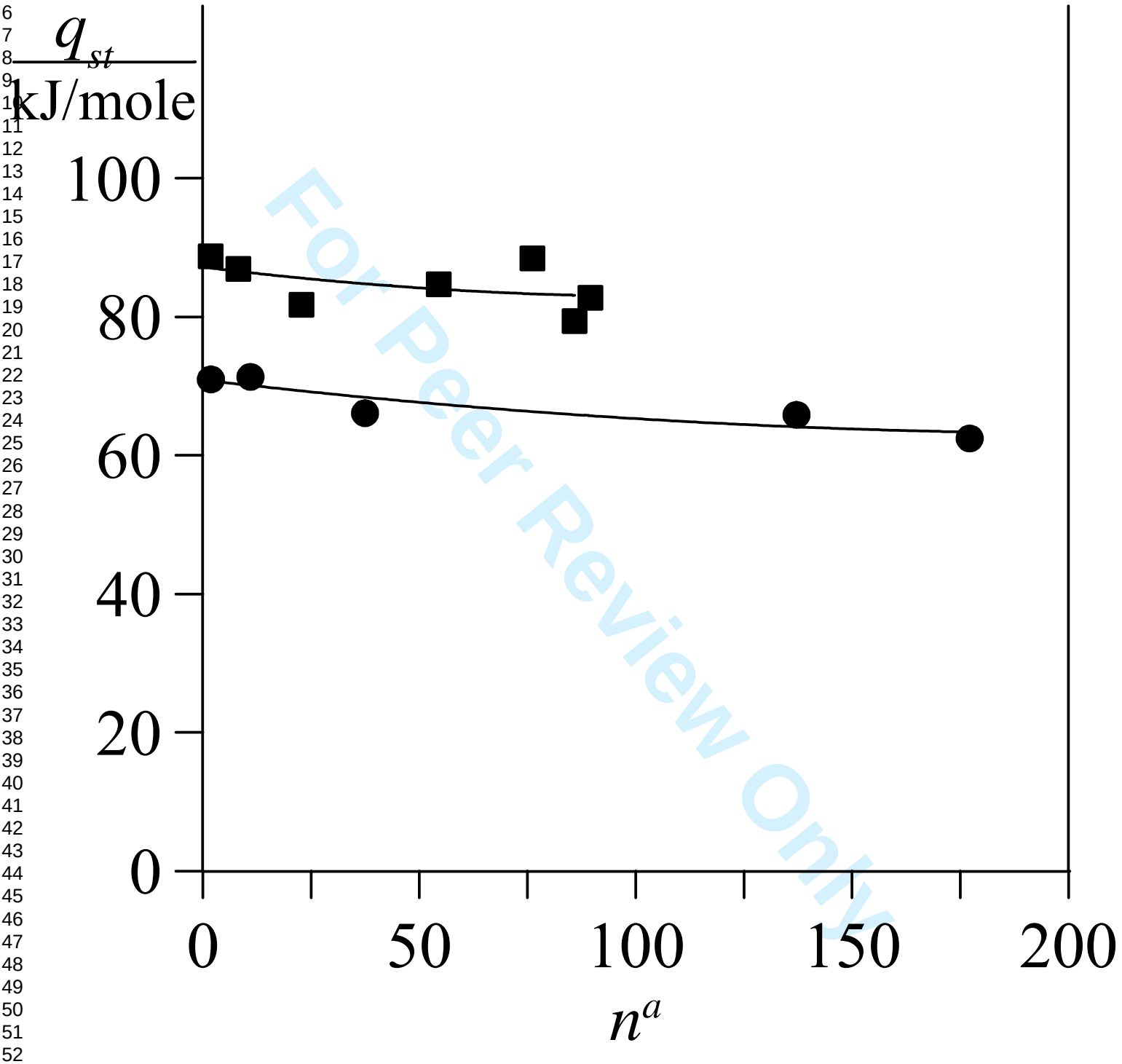

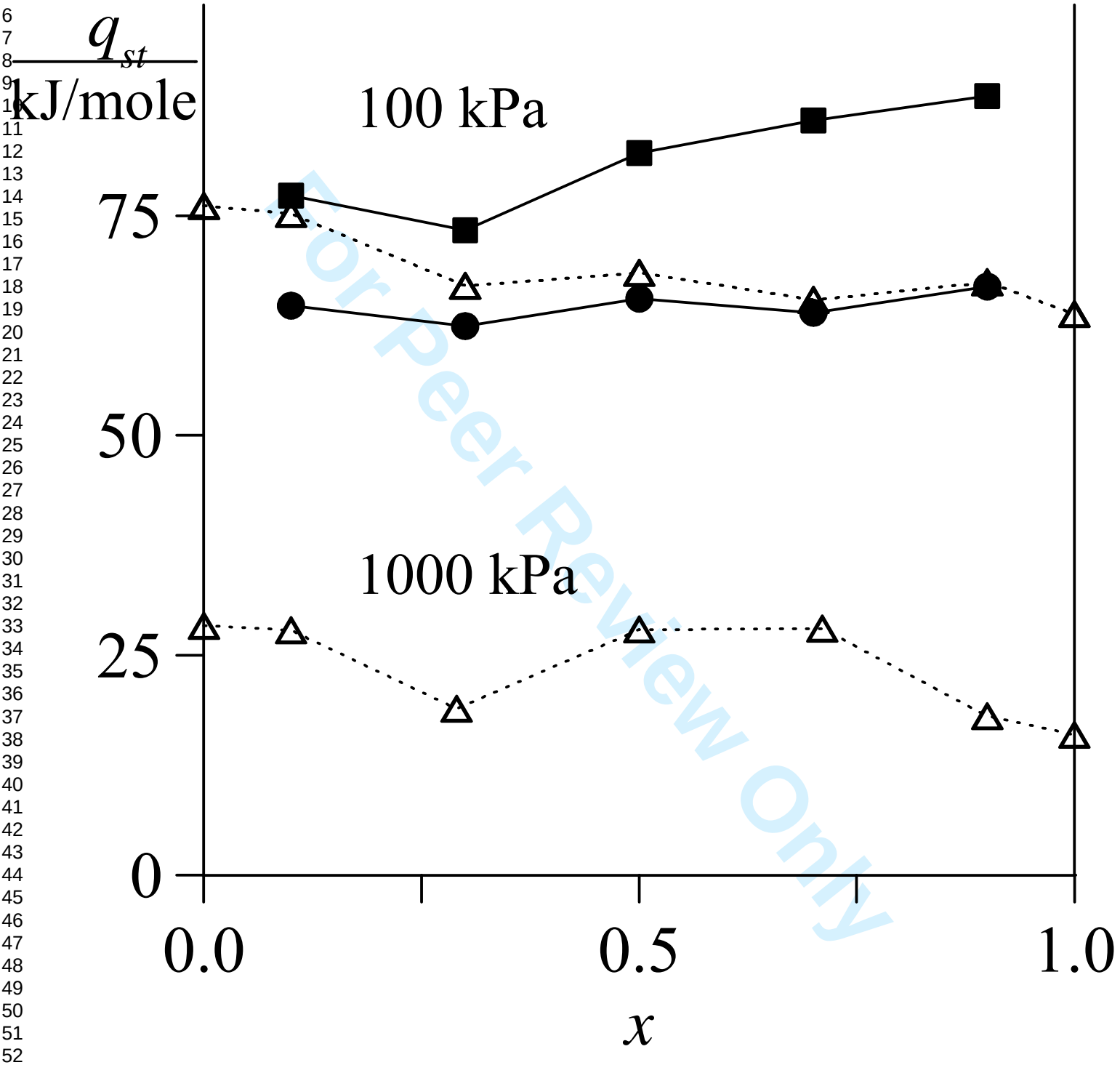

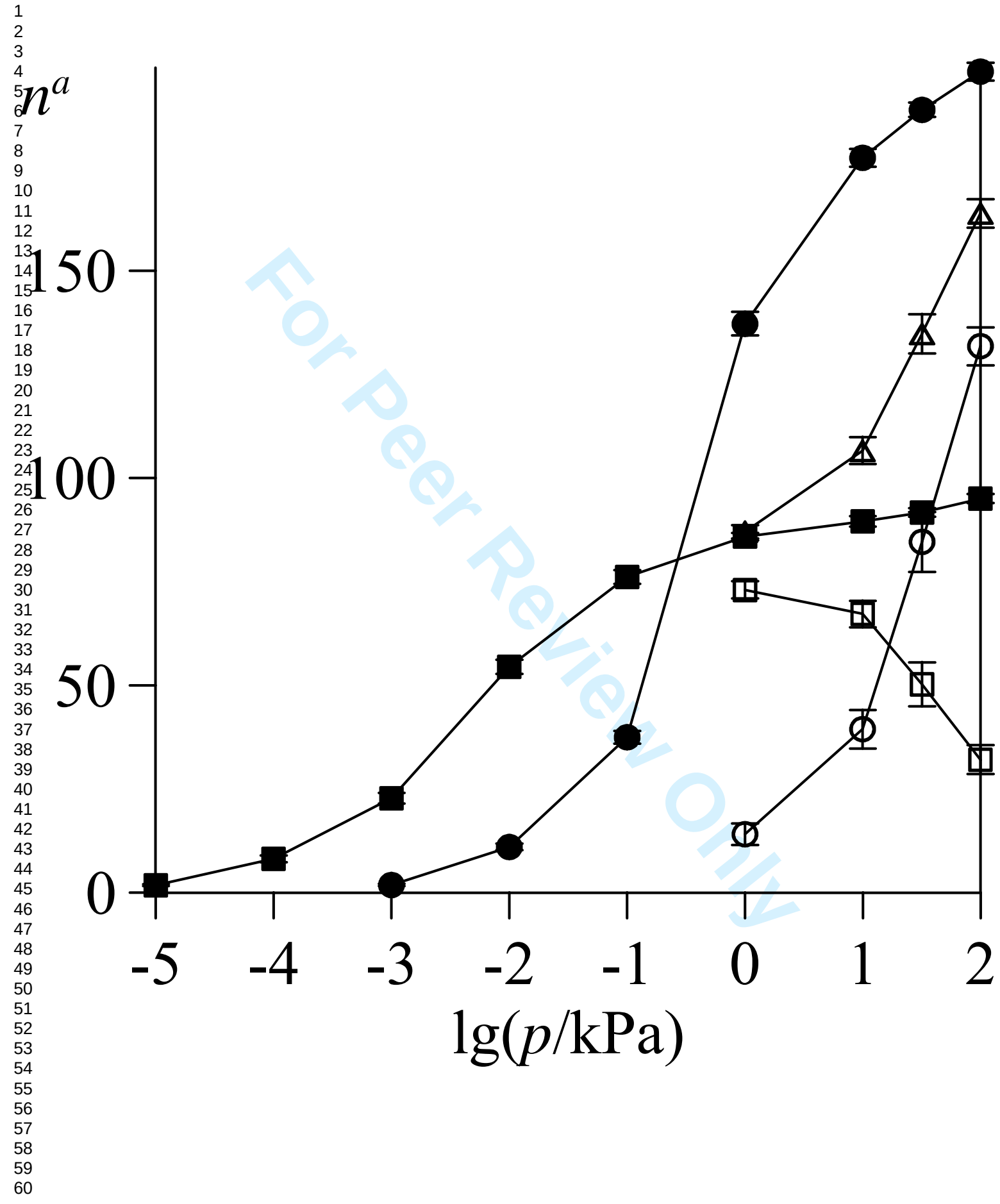

Prediction of adsorption equilibria of water-methanol mixtures in zeolite NaA by molecular simulation

T. KRISTÓF[*†], É. CSÁNYI[†], G. RUTKAI[†] and L. MERÉNYI[‡]

[†]Department of Physical Chemistry, Pannon University, H-8201 Veszprém, P.O. Box 158, Hungary

[‡]Eötvös Loránd Geophysical Institute, H-1145 Budapest, Columbus u. 17–23, Hungary

Predictions for the adsorption of mixtures of water and methanol in zeolite NaA are reported. The pressure dependence of the adsorption properties such as equilibrium amounts of adsorption and isosteric heats of adsorption are calculated at 378 K by molecular simulations using effective pair potential models. These data are also determined for the adsorption from liquid mixtures. The models predict selectivity inversion in the investigated range of pressure. The change in adsorption ratios can partly be explained by the structural characteristics of the system.

Keywords: mixture adsorption; molecular simulation; selectivity

[*]Corresponding author. E-mail: kristoft@almos.vein.hu

1. Introduction

Zeolites have attracted considerable attention in recent decades due to their potential application as adsorbents, catalysts, ion exchangers, sensors, etc [1, 2]. Zeolites are good candidates for selective membranes because of the adsorption and molecular sieve properties of their unique pore system. The strict distribution of pore sizes and the high regularity of the structure distinguish zeolites from other porous materials, and make possible their high selectivity in separation and catalytic processes. Zeolite membranes have advantages over other types of membranes: they can withstand high temperatures and harsh chemical environments. Zeolite membranes are applied, e.g., for removal of organic compounds from water. Using membranes, better separations can be achieved than by distillation, the process demands substantially less energy and has the ability to separate azeotropic mixtures. Zeolite NaA membranes are known to be outstanding materials for solvent dehydration by pervaporation (in pervaporation, a liquid contacts the membrane and a vapour leaves the permeate side) [3]. In a water/alcohol separation study, Okamoto et al. [3] found that zeolite NaA membranes showed a high permselectivity of water to alcohols. The separation factors for the alcohol-water mixtures were in the order: n-propanol > ethanol > methanol. The separation efficiency of such membranes depends on the surface properties (hydrophobicity and hydrophilicity) and the pore dimensions with respect to the molecular sizes. The effect of confinement on molecules contacting zeolites is a complex problem; not only the adsorption selectivity, but also the difference between the diffusivities of the mixture components determines permselectivity.

Deleted: 1

In the past few years, molecular modelling and simulations have been widely applied to study porous materials, as well as the static and dynamic properties of fluids confined in pores [4, 5]. In spite of that fully atomistic simulations of zeolites (sorption and diffusion phenomena in zeolites) are expensive, a number of works have been devoted to simulating these systems as realistically as possible [6-9] to probe experimentally inaccessible properties and to understand the relationship between microscopic and macroscopic characteristics of these systems. There are many simulation studies on pure component and mixture adsorptions in zeolites, including the adsorption of small gas molecules [10, 11], water [12], as well as linear, branched and cyclic alkanes [13-14]. However, the separation of water from organic compounds by selective adsorption in zeolites has received less attention. Recently, water/ethanol adsorption in zeolite NaA has been investigated by Furukawa et al. [16]. These authors found high adsorption selectivity for water, which is consistent with the fact that the highly polar water molecules have more pronounced interactions with the crystal.

This paper presents simulation results for the adsorption from binary mixtures of water and methanol in zeolite NaA. To investigate the driving forces behind selectivity, the pressure dependence of the adsorption properties is analyzed using atomistically detailed microstructure for the adsorbent.

Deleted: 2
Deleted: 3
Deleted: ,
Deleted: 4
Deleted: 7
Deleted: 8
Deleted: 9
Deleted: 0
Deleted: 1
Deleted: 3
Deleted: 4
Deleted: than with the ethanol molecules

2. Models and methodology

Zeolites are tectoaluminosilicates and their crystalline structures consist of tetrahedral TO_4 with T being the tetrahedral atom, Al or Si at the centre of the tetrahedron. The general formula of zeolites can be written as $M_{x/n}[(AlO_2)_x(SiO_2)_y]$, where extra framework cations M, of valence n, neutralize negative charges on the aluminosilicate framework. In zeolite NaA the basic tetrahedral units are organized into secondary units, such as 4R, 6R and 8R rings, where the number of O (or Si/Al) atoms is equal to 4, 6 and 8, respectively. An interconnection of 4R and 6R rings yields nearly spherical cages, known as sodalite cages, which are joined by O bridges on the 4R rings to form a cubic arrangement of cavities (supercages) in the three-dimensional network of this zeolite [17]. The diameter of the supercages is approximately 1.2 nm, and each one is connected to 6 neighbouring supercages with 8R windows of diameter about 0.45 nm. The $fm\bar{3}c$ space group represents the crystal structure with a lattice parameter of 2.4555 nm. The unit cell composition of the crystal is chosen for the present study so that the Si/Al ratio is 1.0. In this way, the obtained unit cell contains 96 Na^+ ions, 96 Si, 96 Al and 384 O atoms with alternating SiO_4 and AlO_4 tetrahedra (according to the Löwenstein rule that prohibits Al-O-Al linkages), which form 8 sodalite cages as well as 8 supercages. The majority of the extra framework Na^+ ions are rather strongly bound at the centres of 6R windows (one ion per window); the remaining ions oscillate around the centres of 8R windows except for 8 ions that can be found typically inside the supercages in front of the 4R windows [17].

Deleted: 5

Deleted: 5

The models used in earlier simulation studies for the framework are either flexible [18] or rigid [19-22]. In the latter the framework atoms are fixed at their crystallographic positions. In this work, only the Na^+ ions from among the zeolite constituents were allowed to move freely during the simulations, but their starting positions were defined according to the optimized geometry. The potential model is the same as that used by Lee et al. [22]. It combines Lennard-Jones pair potentials with partial point charges. The Lennard-Jones energy (ε) and size (σ) parameters, as well as the point charges are given in table 1. The water and methanol molecules were modelled by the SPC/E model [23] and an OPLS type model [24] proposed by van Leeuwen and Smit [25], respectively (table 2). The Lennard-Jones parameters for interactions between unlike groups were calculated by applying the conventional Lorentz-Berthelot combining rules for both, energy and size parameters; i.e., no adjustable binary interaction parameters were introduced. The long-range corrections for the Lennard-Jones interactions were estimated by assuming that the pair correlation functions have approximately unit values beyond the cut-off radius, r_c [26]. The Coulomb potential energy was calculated by the Wolf method [27], which requires less computation time as compared to the conventional Ewald summation technique [28]. There is a close connection between the Wolf method and the Ewald method, but the Wolf method allows the long-ranged Coulomb interactions to be turned into relatively short-ranged effective potentials by neutralizing the net charge of the system within the volume bounded by the cut-off radius. It was shown [29] that, in most systems of interest, the best reproduction of the results obtained by the Ewald method can be achieved with $r_c = L_{min}/2$

Deleted: 6
Deleted: 7
Deleted: 0
Deleted: fixed
Deleted: 0
Deleted: 1
Deleted: 2
Deleted: 3
Deleted: 4
Deleted: 5
Deleted: 6
Deleted: 7

and $\alpha = 4/L_{min}$, where α is the convergence (damping) parameter of the method and L_{min} is the smallest box length occurring in the simulation.

The adsorption properties were computed using the grand canonical Monte Carlo (MC) method in the zeolite NaA system with a fixed cubic box length of 2.4555 nm (therefore, r_c and α were set to 1.22775 nm and 1.6290 nm, respectively). The length of the simulations was typically in the order of 10^8 MC moves in addition to an equilibration period of at least 8×10^7 MC moves. The respective moves included particle insertions and deletions of 70-80 %. The sampling efficiency was increased by using the configurational-bias technique [30]. Since the models for the adsorbate molecules were assumed to be rigid, in our case the configurational-bias procedure was reduced to selecting m trial orientations for the molecule which is to be inserted or deleted (m was set to 6). Although the acceptance rate of these moves was rather low for the methanol molecules, the convergence of the simulations with mixtures could be drastically improved by employing, to a small percentage of all the attempts, identity change moves (i.e., deletion of a molecule with identity i and insertion of a new molecule with identity j at the same centre-of-mass coordinates) [31]. This MC step was also implemented in conjunction with the orientational-bias procedure. According to our a priori assumption, methanol and water molecules are unable to pass through the windows of the sodalite cage, so it would be unphysical to permit the insertion of molecules inside this cage. In the present simulation study, the physical diffusion pathways in the zeolite were taken into account so that this cage interior might only be accessible through particle displacement moves.

Deleted: and

Deleted: t

Deleted: 28

Deleted: 29

The grand canonical ensemble is ideally suited to the calculation of the isosteric heat of adsorption. The isosteric heat of adsorption can be defined as the difference of the partial molar enthalpy in the bulk phase (isothermal-isobaric conditions) and the derivative of the internal energy with respect to the adsorbate mole number in the adsorbed phase (isothermal-isochoric conditions):

$$q_{st,i} = \left(\frac{\partial H^b}{\partial n_i^b} \right)_{p,T,n_{j\neq i}} - \left(\frac{\partial U^a}{\partial n_i^a} \right)_{V,T,n_{j\neq i}}, \quad (1)$$

where, H and U refer to the residual enthalpy and residual internal energy, respectively, n_i is the mole number of component i, and a and b denote the adsorbed and bulk phases, respectively. For an ideal gas adsorbate, the first term of this expression reduces to RT with R being the gas constant. The second term can be obtained from grand canonical adsorption simulations using the particle number fluctuations and the cross-correlation of potential energy and particle number fluctuations [33, 34].

Deleted: 1

Deleted: 2

3. Results and discussion

Since permeation experiments with alcohol-water mixtures were carried out at atmospheric pressure [3], the maximum pressure in the gas adsorption calculations was taken to be p = 100 kPa. In this case the temperature should be above the normal boiling point of water, and therefore we performed the grand canonical simulations by fixing the temperature at T = 378 K. The chemical potentials, which represent the partial pressures of the adsorbate species in the bulk gas phase at a given temperature, were determined from

Deleted: 1

the ideal gas law. We checked the targeted pressure and composition in the gas phase by separately simulating the gas phase properties in the grand canonical ensemble, and found that the deviation from ideal gas behaviour is generally smaller than 2 %. As we verified by additional simulations that the necessary modifications of chemical potential would result in negligible changes in the calculated adsorption properties, we considered the ideal gas approximation to be satisfactory under the thermodynamic conditions used in the gas adsorption calculations.

Adsorption from liquid mixtures was also simulated at T = 378 K; with this system, p = 1000 kPa is sufficient to achieve liquid phase conditions at this temperature. For a given composition, the appropriate chemical potentials were determined from simultaneous grand canonical and semigrand canonical [32] simulations in the liquid phase. We needed both simulation methods for tuning the pairs of chemical potentials, because at the expected high densities the grand canonical method provides the system pressure with large statistical uncertainties. In contrast, the semigrand canonical method enables the simulation to be performed at fixed pressure, but operates with the difference of the chemical potentials only.

To test the validity of the potential models, first we conducted adsorption simulations with pure gases at T = 298 K, where experimental adsorption isotherms are available [3]. Figure 1 shows the calculated amounts of adsorption and their comparison with experimental results. The relatively good reproduction of the experimental water adsorption is clearly seen. At the same time, the real extent of overestimation of the amounts of adsorption for methanol can be taken to be uncertain when considering the exceptionally large experimental value at about p = 3 kPa. It should be noted that Na^+ ions in the 6R windows

Deleted: 0

Deleted: 1

of the zeolite did not move noticeably during the simulations and they prevented the adsorbate molecules from penetrating into the sodalite cages by particle displacement moves. This observation, which verifies our a priori assumption, was confirmed by performing extremely long simulations at T = 378 K. There is some disagreement in literature concerning the accessibility of sodalite cage, but for molecules greater than water the inaccessibility of this cage interior seems to be evident. However, our results for pure water contradict several experimental observations (see, e.g., ref. [35]), and this may indicate some inadequacy of the zeolite model.

The key simulation results, representing the equilibrium amounts of adsorption versus the bulk phase composition at T = 378 K, are depicted in figure 2. The figure also shows the equilibrium selectivity defined as

$$S = \frac{n^a_{H_2O} / n^a_{CH_3OH}}{n^b_{H_2O} / n^b_{CH_3OH}}, \qquad (2)$$

where the mole number of adsorption n^a is equivalent to the number of adsorbate molecules per unit cell. Considering the gas adsorption curves, the adsorbed amount of water increases significantly when its composition in the gas phase is increased. Qualitatively the same holds for methanol. On the other hand, S decreases with decreasing pressure, i.e. with reducing degree of pore filling. In agreement with experimental observation [3], at ambient pressure the simulation results show adsorption selectivity of this zeolite in favour of water. Between p = 100 kPa and 10 kPa, however, S becomes smaller than 1 for all gas phase compositions. A plausible explanation for such a reversal effect is that at low loadings the adsorbent-adsorbate interactions are relatively stronger for the methanol molecules, while at high loadings the smaller water molecules can more efficiently be packed in confined

Deleted: 3

Deleted: 1

geometries. The density distributions of molecules computed at low and high pressures suggest that the supercages are generally filled in two steps: the adsorbates are initially located near the cage "wall" at about 0.4 nm from the centre (oxygen-centre distance). At low pressures the second step is absent, and the middle region remains unfilled. Therefore, the adsorbent-adsorbate interactions dominate the system. The adsorbent-adsorbate affinity can be characterized by the isosteric heat of adsorption at zero coverage. Figure 3 illustrates the significant difference between the isosteric heats of adsorption in the limit of infinite dilution; at low pressures the zeolite strongly favours the binding of methanol molecules. Returning to figure 2., the most striking feature of the adsorption curves at 1000 kPa is the relatively low adsorption ratio of water: the adsorbed amount of water exceeds that of methanol only at high water contents of the bulk liquid. At the same time, the competition effects between both components are lower compared to the gas adsorption at ambient and moderate pressures. The tendency of selectivity observed here implies that the water-water and water-methanol interaction strengths are weaker in the adsorbed phase at 1000 kPa. At this pressure, the contribution of the bulk phase enthalpy term to the isosteric heat of adsorption is much more significant than that for gas adsorption, and should be calculated from the grand canonical and semigrand canonical [32] simulations completed in the liquid phase. It is noteworthy that the error in q_{st} introduced by assuming ideal gas adsorbate in the current gas adsorption calculations remains in the order of 1 kJ/mol. Figure 4 shows a comparison between the mean heats of adsorption obtained at 100 kPa (gas adsorption) and those obtained for adsorption from liquid. Although the q_{st} values calculated from the fluctuation method exhibit considerable scatter, the difference between the two sets of results can be taken to be approximately equal to the heat of vaporization for these mixtures

Deleted: 0

(at this temperature, the heat of vaporization is slightly higher and lower than 40 kJ/mol for water and methanol, respectively). A rough estimation of the adsorbate number densities within the supercages also confirms that the adsorbates are, at both pressures, in a quasi-liquid state. Considering also the results obtained at lower pressures down to 1 kPa (these data are not plotted here), it can be ascertained that the net heat of adsorption, i.e. the difference between the heat of adsorption and the heat of vaporization, only very slightly changes with loading. This behaviour indicates that the decrease of adsorbent-adsorbate interactions with increasing loading is counterbalanced by the increase of adsorbate-adsorbate interactions. As demonstrated in figure 5, at this temperature the expected condensation occurs already below 1 kPa. At lower pressures, more methanol molecules enter the supercages. At higher pressures, water molecules form more water-water hydrogen bonding, and displace methanol molecules out of the pores.

Deleted: s

Deleted: initially

The adsorbate-adsorbate pair correlation functions for O-O, O-H and H-H pairs calculated at low degrees of pore filling indicate that the adsorbed molecules show a structure intermediate between that of bulk liquid and that of bulk gas. These site-site pair correlation functions computed when the pores are filled confirm the above conclusion that the confined mixtures have a structure that does not differ significantly from that of bulk liquid mixtures. This is demonstrated in figure 6 in the case of O-H pairs: the positions of the main peaks are the same in the adsorbed phase and in the bulk. Here, the intensity of the first peaks indicates rather strong adsorbate-adsorbate hydrogen bonding (the plotted functions are normalized to the corresponding total number of adsorbed molecules for comparison). Moreover the curves clearly show the importance of water-water hydrogen

bonding, compared with that of methanol-methanol hydrogen bonding, in the adsorbed phase.

For all pressures, the adsorbent-adsorbate pair correlation functions for Na-O pairs are comparatively featureless except for an intense peak at about 0.25 nm, which are more pronounced in the case of methanol. This reflects strong cation-methanol and somewhat weaker cation-water interactions. At the same time, comparing the corresponding functions for the adsorbate-adsorbate and adsorbent-adsorbate O-H pairs, the hydrogen bonding between the adsorbates and the O site of the adsorbent was found to be quite weak for methanol and only slightly stronger for water. The methanol-adsorbent and water-adsorbent pair correlation functions for O-O sites are similar in that a very sharp (first) peak is absent. Figure 7 shows these functions at two different pressures, between which selectivity inversion occurs at equimolar composition of the gas phase. For mixture adsorption, this plot demonstrates that adsorbed water is more structured than adsorbed methanol. Water molecules can get closer to the lattice sites, and this indirectly reflects also their greater hydrogen bonding ability. At higher loading the decrease in mean molecule size, which occurs when methanol is replaced by water, is favoured. For pure component adsorption, this is not the case. The first peak is more pronounced and its distance is smaller in the case of methanol, which indicates that methanol molecules have greater affinity to the adsorbent. Here, the higher degree of adsorption of water compared to methanol highlights the significance of strong water-water interactions induced by the confinement of molecules within the supercages.

Deleted: The adsorbent-adsorbate pair correlation

Deleted: for O-O sites

Deleted: , are presented in figure 6

Deleted: For comparison, all these functions are normalized to the corresponding total number of adsorbed molecules.

4. Conclusion

Predictions for the adsorption of binary mixtures of water and methanol in zeolite NaA are presented at 378 K for a number of different bulk phase compositions using effective pair potential models in molecular simulations. Equilibrium amounts of adsorption and isosteric heats of adsorption are calculated in a wide range of bulk phase pressure including the liquid phase region. In agreement with experimental observation, at ambient pressure the models predict significantly higher equilibrium selectivity for water. However, the competition between entropic and energetic effects leads to complex behaviour of the system. Reducing the pressure, selectivity inversion occurs. Our calculations show that the adsorbent-adsorbate interactions, which control the properties of the system at low loadings, are stronger for methanol. Surprisingly, a reversal of selectivity also takes place on passing from the bulk gas phase to the bulk liquid phase region. We conclude that at least two factors influence principally the adsorption ratio at higher pressures. Because water and methanol molecules have comparable dipole moments but different sizes, steric rather than electrostatic interactions should become dominant in the zeolit pores as the pressure increases. In parallel with this, water-water interactions due to hydrogen bonding become stronger in the adsorbed phase but also in the bulk phase, and the presence of strong hydrogen bonding in liquid water partially hinders the water adsorption from liquid.

Given the sensitive manner in which the calculated selectivities depend on the model parameters, it will be interesting to determine the range of selectivity inversion by using other (or modified) realistic potential models. Such analysis is currently in progress.

Deleted: ,

Deleted: to such an extent that

Acknowledgements

This work has been supported by the Hungarian Scientific Research Fund (Grant No. OTKA K 63322).

REFERENCES

[1] H. van Bekkum, E. M. Flaningen, J. C. Jansen (Eds.). *Introduction to Zeolite Science and Practice,* Elsevier, Amsterdam (1991).

[2] S. M. Auerbach, K. A. Carrado, P. K. Dutta (Eds.). *Handbook of zeolite science and technology,* Dekker, New York (2003).

[3] K. Okamoto, H. Kita, K. Horii, K. Tanaka, M. Kondo. Zeolite NaA Membrane: Preparation, Single-Gas Permeation, and Pervaporation and Vapor Permeation of Water/Organic Liquid Mixtures. *Ind. Eng. Chem. Res.*, **40**, 163 (2001).

[4] K. E. Gubbins, N. Quirke (Eds.). *Molecular Simulation and Industrial Applications: Methods, Examples and Prospects,* Gordon & Breach, Amsterdam (1997).

[4] B. Smit, R. Krishna. Molecular simulations in zeolitic process design. *Chem. Eng. Sci.*, **58**, 557 (2003).

[6] C. P. Herrero. Monte Carlo Simulation of the Si, Al Distribution in A-Type Zeolites. *J. Phys. Chem.*, **97**, 3338 (1993).

[7] K.-P. Schröder, J. Sauer. Potential Functions for Silica and Zeolite Catalysts Based on ab Initio Calculations. 3. A Shell Model Ion Pair Potential for Silica and Aluminosilicates. *J. Phys. Chem.*, **100**, 11043 (1996).

[8] D. Nicholson, R. J.-M. Pellenq. Adsorption in zeolites: intermolecular interactions and computer simulation. *Adv. Colloid Interface Sci.*, **76-77**, 179 (1998).

[9] D. Dubbeldam, S. Calero, T. J. H. Vlugt, R. Krishna, T. L. M. Maesen, E. Beerdsen, B. Smit. Force Field Parametrization through Fitting on Inflection Points in Isotherms. *Phys. Rev. Lett.*, **93**, 088302 (2004).

Deleted: 1

Deleted: 2

Deleted: 3

Deleted: 4

Deleted: 5

Deleted: 6

Deleted: 7

[10] T. J. Grey, D. Nicholson, J. D. Gale, B. K. Peterson. A simulation study of the adsorption of nitrogen in Ca-chabazite. *Appl. Surf. Sci.*, **196**, 105 (2002).

[11] G. Maurin, Ph. Llewellyn, Th. Poyet, B. Kuchta. Influence of Extra-Framework Cations on the Adsorption Properties of X-Faujasite Systems: Microcalorimetry and Molecular Simulations. *J. Phys. Chem. B*, **109**, 125 (2005).

[12] C. E. Ramachandran, S. Chempath, L. J. Broadbelt, R. Q. Snurr. Water adsorption in hydrophobic nanopores: Monte Carlo simulations of water in silicalite. *Microporous Mesoporous Mat.*, **90**, 293 (2006).

[13] B. Smit, R. Krishna. Monte Carlo simulations in zeolites. *Current Opinion Sol. State Mat. Sci.*, **5**, 455 (2001).

[14] P. Pascual, A. Boutin, P. Ungerer, B. Tavitian, A. H. Fuchs. Adsorption of Linear Alkanes in Zeolite Ferrierite from Molecular Simulations. *Mol. Sim.*, **30**, 593 (2004).

[15] J. P. Fox, S. P. Bates. Simulating the Adsorption of Binary and Ternary Mixtures of Linear, Branched, and Cyclic Alkanes in Zeolites. *J. Phys. Chem. B*, **108**, 17136 (2004).

[16] S. Furukawa, K. Goda, Y. Zhang, T. Nitta. Molecular Simulation Study on Adsorption and Diffusion Behavior of Ethanol/Water Molecules in NaA Zeolite Crystal. *J. Chem. Eng. Japan*, **37**, 67 (2004).

[17] J. J. Pluth, J. V. Smith. Accurate Redetermination of Crystal Structure of Dehydrated Zeolite A. Absence of Near Zero Coordination of Sodium. Refinement of Si,Al-Ordered Superstructure. *J. Am. Chem.. Soc.*, **102**, 4704 (1980).

[18] D. A. Faux, W. Smith, T. R. Forester. Molecular Dynamics Studies of Hydrated and Dehydrated Na^+-Zeolite-4A. *J. Phys. Chem. B*, **101**, 1762 (1997).

Deleted: 8

Deleted: 9

Deleted: 0

Deleted: 1

Deleted: 2

Deleted: 3

Deleted: 4

Deleted: 5

Deleted: 6

[19] E. C. DeLara, R. Kahn, A. M. Goulay. Molecular Dynamic by Numerical Simulation in Zeolites: Methane in NaA. *J. Chem. Phys.*, **90**, 7482 (1989).

[20] S. Bandyopadhyay, S. Yashonath. Anomalous Behaviour of Cage-to-Cage Diffusion of Methane in Zeolits A and Y. *Chem. Phys. Lett.*, **223**, 363 (1994).

[21] C. J. Jameson, A. K. Jameson, B. I. Baello, H. M. Lim. Grand Canonical Monte Carlo Simulations on the Distribution and Chemical Shifts of Xenon in the Cages of Zeolite NaA: I. Distribution and ^{129}Xe Chemical Shifts. *J. Chem. Phys.*, **100**, 5965 (1994).

[22] S. H. Lee, G. K. Moon, S. G. Choi, H. S. Kim. Molecular Dynamics Simulation Studies of Zeolite-A. 3. Structure and Dynamics of Na^+ Ions and Water Molecules in a Rigid Zeolite-A. *J. Phys. Chem.*, **98**, 1561 (1994).

[23] H. J. C. Berendsen, J. R. Grigera, T. P. Straatsma. The Missing Term in Effective Pair Potentials. *J. Phys. Chem.*, **91**, 6269 (1987).

[24] W. L. Jorgensen. Optimized Intermolecular Potential Functions for Liquid Alcohols. *J. Phys. Chem.*, **90**, 1276 (1986).

[25] M. E. van Leeuwen, B. Smit. Molecular simulation of the Vapor-Liquid Coexistence Curve of Methanol. *J. Phys. Chem.*, **99**, 1831 (1995).

[26] M. P. Allen, D. J. Tildesley. *Computer Simulation of Liquids*, Clarendon, Oxford (1987).

[27] D. Wolf, P. Keblinski, S. R. Phillpot, J. Eggebrecht. Exact method for the simulation of Coulombic systems by spherically truncated, pairwise r^{-1} summation. *J. Chem. Phys.*, **110**, 8254 (1999).

[28] S. W. de Leeuw, J. W. Perram, E. R. Smith. Simulation of electrostatic systems in

Deleted: 7

Deleted: 18

Deleted: 19

Deleted: 0

Deleted: 1

Deleted: 2

Deleted: 3

Deleted: 4

Deleted: 5

Deleted: 6

periodic boundary conditions: I. Lattice sums and dielectric constants. *Proc. R. Soc. London A*, **A373**, 27 (1980).

[29] P. Demontis, S. Spanu, G. B. Suffritti. Application of the Wolf method for the evaluation of Coulombic interactions to complex condensed matter systems: Aluminosilicates and water. *J. Chem. Phys.*, **114**, 7980 (2001).

[30] J. I. Siepmann, D. Frenkel. Configurational Bias Monte Carlo: a New Sampling Scheme for Flexible Chains. *Mol. Phys.*, **75**, 59 (1992).

[31] D. A. Kofke, E. D. Glandt. Monte Carlo simulation of multicomponent equilibria in a semigrand canonical ensemble. *Mol.Phys.*, **64**, 1105 (1988).

[32] D. Frenkel, B. Smit. *Understanding Molecular Simulation*, Academic Press, San Diego (1996).

[33] D. Nicholson, N. G. Parsonage. *Computer Simulation and the Statistical Mechanics of Adsorption*; Academic Press, London (1982).

[34] F. Karavias, A. L. Myers. Isosteric Heats of Multicomponent Adsorption: Thermodynamics and Computer Simulations. *Langmuir*, **7**, 3118 (1991).

[35] J. C. M. Müller, G. Hakvoort, J. C. Jansen. DSC and TG study of water adsorption and desorption on zeolite NaA. *J. Therm. Anal.*, **53**, 449 (1998).

Deleted: 7

Deleted: 28

Deleted: 29

Deleted: 0

Deleted: 1

Deleted: 2

Deleted: 3

Tables

Table 1. Lennard-Jones energy (ε) and size parameters (σ) as well as partial charges (q) for zeolite NaA [22].

	Na^+	Si	Al	O^1	O^2	O^3
ε/k_B (K)	2507.3	64.18	64.18	78.02	78.02	78.02
σ (nm)	0.1776	0.4009	0.4009	0.2890	0.2890	0.2890
q (electron charge)	0.5502	0.6081	0.6081	-0.4431	-0.4473	-0.4380

[1] member of 4R and 8R
[2] member of 6R and 8R
[3] member of 4R and 6R

Table 2. Lennard-Jones energy (ε) and size parameters (σ), partial charges (q) and geometry data (bond length δ and bond angle β) for water and methanol.

	ε_O/k_B (K)	ε_{CH_3}/k_B (K)	σ_O (nm)	σ_{CH_3} (nm)	q_O (electron charge)	q_{CH_3} (electron charge)	q_H (electron charge)	$\delta_{O\text{-}CH_3}$ (nm)	$\delta_{O\text{-}H}$ (nm)	$\beta_{H\text{-}O\text{-}(C)H_{(3)}}$
SPC/E water [23]	78.197	-	0.3166	-	-0.8476	-	0.4238	-	0.1000	109.47°
OPLS methanol [25]	86.50	105.2	0.303	0.374	-0.700	0.265	0.435	0.1425	0.0945	108.53°

Figure captions

Fig. 1. Adsorption isotherms of water (circles) and methanol (squares) on zeolite NaA at 298 K. n^a is the number of adsorbate molecules per unit cell. Open and closed symbols correspond to adsorption and desorption experiments, respectively. The statistical uncertainties of the simulation results (crossed symbols) do not exceed the symbol size.

Fig. 2. Simulated amounts of adsorption and selectivities for water-methanol mixtures on zeolite NaA at 378 K. x refers to the mole fraction of water in the bulk phase, n^a is the number of adsorbate molecules per unit cell. The circles and squares correspond to water and methanol, respectively; the triangles represent the equilibrium selectivities.

Fig. 3. Simulation results for isosteric heat of adsorption as a function of coverage on zeolite NaA at 378 K. n^a is the number of adsorbate molecules per unit cell. The circles and squares correspond to water and methanol, respectively.

Fig. 4. Simulation results for isosteric heat of adsorption on zeolite NaA at 378 K. x refers to the mole fraction of water in the bulk phase. The circles and squares correspond to water and methanol, respectively; the triangles represent the mean isosteric heats.

Fig. 5. Adsorption isotherms of water (circles) and methanol (squares) on zeolite NaA at 378 K. n^a is the number of adsorbate molecules per unit cell. Closed symbols correspond to

the pure components, open symbols stand for these components at equimolar composition of the gas phase. The triangles indicate the total loadings for the mixture adsorption.

Fig. 6. O-H pair correlation functions for approximately equimolar water-methanol mixtures at 378 K. Light-coloured and dark curves represent the results obtained in the adsorbed phase at 100 kPa and in the bulk liquid phase at 1000 kPa, respectively. Note that the densities of the two systems are different. The solid, dashed and dotted lines correspond to the water-water, methanol-methanol and water-methanol interactions, respectively.

Deleted: 6

Fig. 7. O(zeolite)-O(adsorbate) pair correlation functions for adsorption from pure water and pure methanol gases (upper curves that converge to unity) and from equimolar water-methanol gas mixtures (lower curves that converge to the corresponding adsorbate mole fractions) at 378 K. Light-coloured and dark curves represent the results obtained at 10 and 31.62 kPa, respectively. The solid lines correspond to the O site of water and the dashed lines correspond to that of methanol.